Toxicology and Applied Pharmacology xxx (2016) xxx–xxx

Contents lists available at ScienceDirect

Toxicology and Applied Pharmacology

journal homepage: www.elsevier.com/locate/ytaap

Reduction of hexavalent chromium by fasted and fed human gastric fluid. II. *Ex vivo* gastric reduction modeling

Christopher R. Kirman [a], Mina Suh [b], Sean M. Hays [c], Hakan Gürleyük [d], Russ Gerads [d], Silvio De Flora [e], William Parker [f], Shu Lin [f], Laurie C. Haws [g], Mark A. Harris [h], Deborah M. Proctor [b,*]

[a] *Summit Toxicology, Orange Village, OH, 44022, USA*
[b] *ToxStrategies, Inc., Mission Viejo, CA, 92692, USA*
[c] *Summit Toxicology, Allenspark, CO, 8040, USA*
[d] *Brooks Applied Labs, Bothell, WA, 98011, USA*
[e] *Department of Health Sciences, University of Genoa, 16132 Genoa, Italy*
[f] *Duke University Medical Center, Department of Surgery, Durham, NC, 27710, USA*
[g] *ToxStrategies, Inc., Katy, TX, 77494, USA*
[h] *ToxStrategies, Inc., Austin, TX, 78751, USA*

ARTICLE INFO

Article history:
Received 5 April 2016
Revised 29 June 2016
Accepted 4 July 2016
Available online xxxx

Keywords:
Hexavalent chromium
stomach reduction kinetics
human gastric fluid
Speciated Isotope Dilution Mass Spectrometry (SIDMS)

ABSTRACT

To extend previous models of hexavalent chromium [Cr(VI)] reduction by gastric fluid (GF), *ex vivo* experiments were conducted to address data gaps and limitations identified with respect to (1) GF dilution in the model; (2) reduction of Cr(VI) in fed human GF samples; (3) the number of Cr(VI) reduction pools present in human GF under fed, fasted, and proton pump inhibitor (PPI)-use conditions; and (4) an appropriate form for the pH-dependence of Cr(VI) reduction rate constants. Rates and capacities of Cr(VI) reduction were characterized in gastric contents from fed and fasted volunteers, and from fasted pre-operative patients treated with PPIs. Reduction capacities were first estimated over a 4-h reduction period. Once reduction capacity was established, a dual-spike approach was used in speciated isotope dilution mass spectrometry analyses to characterize the concentration-dependence of the 2nd order reduction rate constants. These data, when combined with previously collected data, were well described by a three-pool model (pool 1 = fast reaction with low capacity; pool 2 = slow reaction with higher capacity; pool 3 = very slow reaction with higher capacity) using pH-dependent rate constants characterized by a piecewise, log-linear relationship. These data indicate that human gastric samples, like those collected from rats and mice, contain multiple pools of reducing agents, and low concentrations of Cr(VI) (<0.7 mg/L) are reduced more rapidly than high concentrations. The data and revised modeling results herein provide improved characterization of Cr(VI) gastric reduction kinetics, critical for Cr(VI) pharmacokinetic modeling and human health risk assessment.

1. Introduction

Drinking water consumption of high concentrations (5 to 180 mg/L) of hexavalent chromium [Cr(VI)] has been found to produce tumors in the small intestines of mice following lifetime oral exposures (NTP, 2008). However, it has been recognized for several decades that Cr(VI) can be detoxified via extracellular reduction to inert trivalent chromium [Cr(III)] in the gastrointestinal lumen (De Flora et al., 1987; De Flora, 2000). Characterization of the rates and capacities for Cr(VI) reduction by gastric fluid (GF) prior to reaching critical target tissues in the small intestine (i.e., intestinal mucosa cells) is important for informing extrapolations of toxicity observed across species and for understanding the potential cancer risk posed by environmental exposure to Cr(VI) in the drinking water supply. The rate of Cr(VI) reduction can be described by the following generalized equation:

$$Rate of Reduction\ (mg/hr) = C_{CrVI} \times \left[(K_{Red} \times C_{RE})_{Pool\ 1} + \ldots (K_{Red} \times C_{RE})_{Pool\ N}\right] \quad (1)$$

Where K_{Red} is a second order rate constant for reduction (L^2/mg-hr) for a specific pool of reducing equivalents, C_{RE} is the concentration of reducing equivalents or reduction capacity (mg/L) for a specific pool of reducing agents, C_{CrVI} is the concentration of Cr(VI) (mg/L), and N is the number of pools; and values for K_{Red} and C_{RE} differ between pools (i.e.,

* Corresponding author.
E-mail addresses: ckirman@summittoxicology.com (C.R. Kirman), msuh@toxstrategies.com (M. Suh), shays@summittoxicology.com (S.M. Hays), hakan@brooksrand.com (H. Gürleyük), russ@brooksrand.com (R. Gerads), sdf@unige.it (S. De Flora), william.parker@duke.edu (W. Parker), shu.lin@duke.edu (S. Lin), lhaws@toxstrategies.com (L.C. Haws), mharris@toxstrategies.com (M.A. Harris), dproctor@toxstrategies.com (D.M. Proctor).

http://dx.doi.org/10.1016/j.taap.2016.07.002
0041-008X/

reduction reactions can occur at different rates, with different capacities). The term reducing equivalent is used here for the sake of simplicity to refer to a pool of three-electron donors needed to reduce Cr(VI) to Cr(III). By collecting and modeling time-course data collected for the reduction of Cr(VI) by GF, we can characterize the rates, capacities, and pH-dependence of the reaction, which is then used in a physiologically based pharmacokinetic model for chromium (Fig. 1).

The capacity of GF for Cr(VI) reduction (C_{RE}) has been characterized in human and animal studies. Based on an *s*-diphenylcarbazide (DPC) colorimetric method, De Flora et al. (1987) reported time-dependent changes in the capacity of GF to reduce Cr(VI) in 16 hospital patients with duodenal ulcer and one healthy volunteer. Shortly after a meal, peak reduction capacities were reported as a single pool ranging from 40 to 60 mg/L, while reduction capacities between meals were generally below 10 mg/L. Confirming the latter value, Kirman et al. (2013) estimated a reduction capacity for a single pool of 7 mg/L in combined GF samples from ten fasted, preoperative cardiac patients using a simple (single, 2nd order reaction) reduction model. Analyzing the same data as Kirman et al. (2013) with a more complex reduction model, Schlosser and Sasso (2014) reported a slightly higher reduction capacity for a single pool of approximately 10 mg/L in fasted human samples. Overall, despite differences in analytical methods or modeling approaches, the capacity estimates for fasted samples from these studies (De Flora et al., 1987; Kirman et al., 2013; Schlosser and Sasso, 2014) are generally consistent. With respect to capacity in GF from laboratory rodents, Proctor et al. (2012) reported that the reduction capacity for GF samples from fed rats and mice was approximately 16 mg/L using a simple, single reduction pool model. Reanalysis of the same data by Schlosser and Sasso (2014) using a multi-pool model, including fast and slow reduction reactions, yielded slightly higher reduction capacities. Specifically, reduction capacities in mouse GF of 2.9 and 31 mg/L for the fast and slow pools, respectively, were reported, while values of 4.1 and 18 mg/L were reported for the fast and slow pools, respectively, in rat GF.

The number of reducing agent pools present in GF (*N* in Eq. (1)) is an important determinant of risk that can affect interspecies extrapolation as well as high-to-low dose extrapolation. In our previous work characterizing the reduction of Cr(VI) by human and rodent GF, we modeled all data using a single-pool model (Proctor et al., 2012; Kirman et al., 2013). Using a revised gastric model, Schlosser and Sasso (2014) relied upon a single-pool model for humans, and a three-pool model for laboratory rodents based upon available *ex vivo* reduction data, and in so doing may have created an apparent species difference (three pools in rodents vs. one pool in humans). However, the single pool used to model the human data may reflect insufficient information that was previously available to allow for differentiation of more than one pool, rather than a true species difference. Specifically, to address the presence of multiple reducing agent pools, GF samples need to be assessed using a wide range of Cr(VI) spike concentrations. In our previous study of human GF (Kirman et al., 2013), a limited number of human fasted samples were used to characterize reduction across different pH values using a fairly narrow range of Cr(VI) spike concentrations. In rodent GF, pH is far less variable than in humans, and we were able to characterize Cr(VI) reduction across a wide range of concentrations (Proctor et al., 2012). Samples were spiked at a range of concentrations representative of the high concentrations used in the rodent cancer bioassay (180 ppm) as well as much lower concentrations consistent with the federal drinking water standard (0.1 ppm).

The reduction of Cr(VI) by human GF is pH dependent, with faster rates of reduction occurring at low pH compared to those at high pH (De Flora et al., 1987; De Flora et al., 2016; Kirman et al., 2013). Similar pH-dependent behaviors have been reported for specific reducing

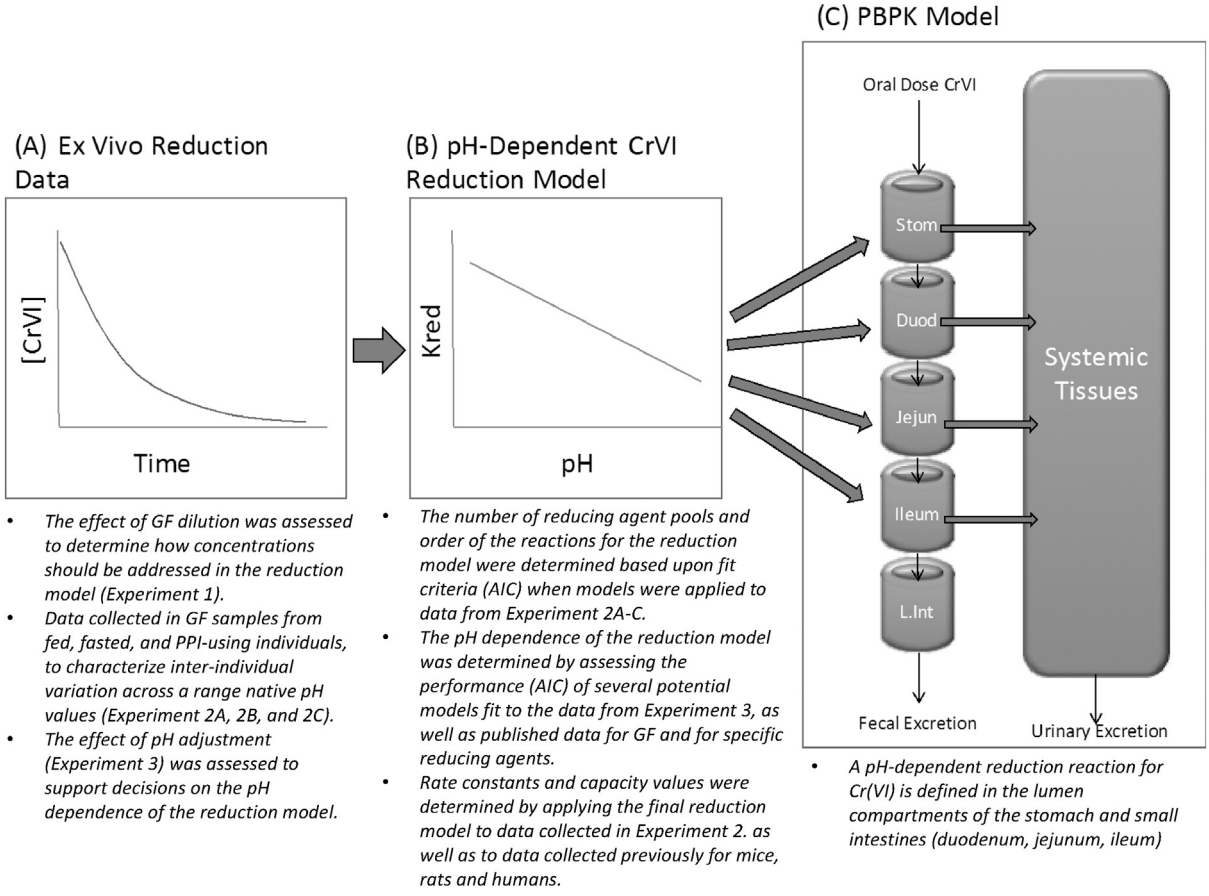

Fig. 1. Role of ex vivo reduction data (A) in developing a reduction model (B) and a PBPK model for Cr(VI) (C).

Please cite this article as: Kirman, C.R., et al., Reduction of hexavalent chromium by fasted and fed human gastric fluid. II. *Ex vivo* gastric reduction modeling, Toxicol. Appl. Pharmacol. (2016), http://dx.doi.org/10.1016/j.taap.2016.07.002

agents that likely serve as constituents of GF, including glutathione (Wiegand et al., 1984) and ascorbate (Dixon et al., 1993). However, the behavior of this pH dependence (i.e., the shape of the reduction constant curve as a function of pH) is less clear. The nature of the pH-dependence for the rate of Cr(VI) reduction serves as an important component of the risk assessment, because it determines the rate of detoxification of Cr(VI) in the stomach between meals (low pH), during meals (short term increase in pH), as well as in potentially sensitive subpopulations with elevated gastric pH levels (e.g., neonates and users of proton pump inhibitors or PPIs). Kirman et al. (2013) assumed an empirical, log-linear relationship between pH and reduction rate constant (*i.e., Kred* from Eq. (1) is expressed as a log-linear function of pH) to help explain the faster reduction rates observed for Cr(VI) at low pH compared to those observed at high pH. Subsequently, Schlosser and Sasso (2014) developed a more complex reduction model to improve the fit of model predictions to the available data. This reduction model included a non-linear relationship between pH and reduction rate based upon a consideration of the predominance of Cr(VI) forms present at a given pH (Fig.

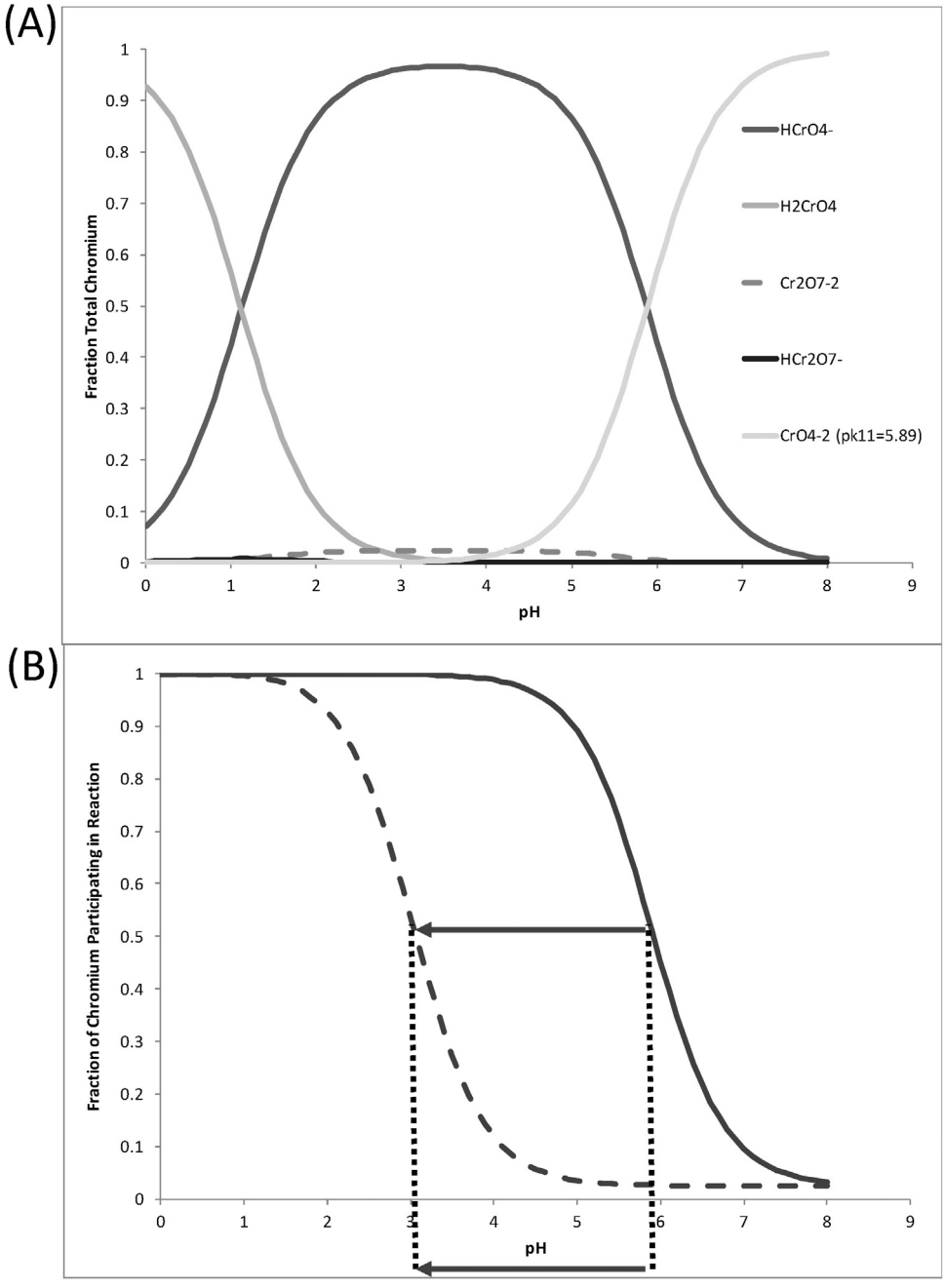

Fig. 2. pH Dependence of Cr(VI) Forms: (A) Showing specific forms of Cr as described by Eqs. (2)-(5) (see text); (B) pH dependence of the predominance model. The fraction of CrVI participating in oxidation/reduction reactions, which is calculated as the sum of all forms of CrVI, with CrO_4^{-2} weighted by a factor of 0.025, as defined by Schlosser and Sasso (2014). The general shape of the pH dependence for this model includes plateaus at observed at pH values above and below an inflection point that is determined by the value of pK11. H_2CrO_4 = dihydrogen chromate; $HCrO_4^-$ = hydrogen chromate; CrO_4^{2-} = chromate; HCr_2O^{7-} = dichromate.

Please cite this article as: Kirman, C.R., et al., Reduction of hexavalent chromium by fasted and fed human gastric fluid. II. *Ex vivo* gastric reduction modeling, Toxicol. Appl. Pharmacol. (2016), http://dx.doi.org/10.1016/j.taap.2016.07.002

2A), with the predominance of the different forms of Cr(VI) defined by the following equations (Brito et al., 1997; Schlosser and Sasso, 2014):

$$CrO_4^{2-} + H^+ \leftrightarrow HCrO_4^-; K_{11} = \frac{[HCrO_4^-]}{[CrO_4^{2-}][H^+]} \quad (2)$$

$$2HCrO_4^- \leftrightarrow Cr_2O_7^{2-} + H_2O; K_{22} = \frac{[Cr_2O_7^{2-}]}{[HCrO_4^-]^2} \quad (3)$$

$$HCrO_4^- + H^+ \leftrightarrow H_2CrO_4; K_{21} = \frac{[H_2CrO_4]}{[HCrO_4^-][H^+]} \quad (4)$$

$$Cr_2O_7^{2-} + H^+ \leftrightarrow HCr_2O_7^-; K_{32} = \frac{[HCr_2O_7^-]}{[Cr_2O_7^{2-}][H^+]} \quad (5)$$

Brito et al. (1997) published the following values to describe chromium speciation equilibria: $K_{11} = 7.73x10^5\ M^{-1}$ ($pK_{11} = 5.89$), $K_{22} = 132\ M^{-1}$ ($pK_{22} = 2.12$), $K_{21} = 13.2\ M^{-1}$ ($pK_{21} = 1.12$), and $K_{32} = 15.2\ M^{-1}$ ($pK_{32} = 1.28$). The forms of Cr(VI) that predominate at low pH have high redox potentials (e.g., H_2CrO_2. $E_0 = +1.33$ V), while the form of Cr(VI) that predominates at high pH has a low redox potential (CrO_4^{2-} E0 = -0.12 V), a pattern that is consistent with a higher rate of Cr(VI) reduction at lower pH than at higher pH. Schlosser and Sasso (2014) have proposed that the pH dependence of Cr(VI) reduction can be attributed the predominance of the form of Cr(VI) present at a given pH (i.e., the C_{CrVI} term in Eq. (1) is replaced by C_{CrVI}*F, in which F is a pH-dependent fraction determined by Eqs. (2)-(5) and depicted in Fig. 2B). However, to achieve fits to the available *ex vivo* reduction data, the predominance model of Schlosser and Sasso (2014) required optimizing the model parameter, K_{11}, resulting in a proposed K_{11} that is shifted by more than two orders of magnitude (e.g., pK_{11} of 3.03 instead of 5.89) (Fig. 2B). Because the K_{11} corresponds to the Ka for chromate, this results in lowering a parameter (Ka) that has been determined with a reasonable degree of certainty from a value of 773,000 to 1,070, which detracts from the chemistry-based approach, making it more of an empirical model.

To date, a number of important limitations and gaps remain regarding Cr(VI) reduction kinetics, including: (1) characterization of Cr(VI) reduction using GF samples from fed individuals (i.e., previous data were largely collected using samples from fasted individuals); (2) characterization of Cr(VI) reduction at elevated pH (i.e., previous data sets were very limited above pH of 4, which greatly hampered the characterization of the pH-dependence for Cr(VI) reduction); and (3) characterization of individual variation in fasted, fed, and PPI samples (i.e., previous data sets relied primarily upon pooled fasted GF samples). The following work describes a series of experiments using samples obtained from De Flora et al. (2016), and kinetic modeling designed to address many of these data gaps and limitations, with the ultimate goal of providing data to support pharmacokinetic modeling and human health risk assessment for Cr(VI) (Fig. 1).

2. Material and Methods

2.1. Gastric Sample Collection and Analysis

GF samples were collected from three groups: (1) eight healthy human volunteers in Italy (n = 8, pH 1.7 to 3.5) who provided pre- and post-meal samples (as described in De Flora et al., 2016); (2) one volunteer who provided a post-meal (vomit) sample (pH 1.8); and (3) three pre-operative patients on PPIs (GF pH 5 to 7.5) at Duke University Hospital who provided fasted samples. For samples in the group 1, only 7/8 fed samples were analyzed, which when combined with the group 2 sample yielded a total of 8 fed samples analyzed. Similarly, only 5/8 fasted samples from group 1 were analyzed. Because the PPI samples were collected from anonymous patients, the Duke University IRB determined that IRB approval (Protocol ID Pro00028884) was not required, and the study satisfied the Privacy Rule as described in 45 CFR 164:514. From the volunteers in Italy, nasogastric tubes were used to collect the gastric samples: pre-meal (fasted) samples were collected after an overnight fast and post-meal (fed) samples were collected 1.5 h after lunch. These samples were centrifuged at 1,000*xg*, and gross food residues were removed (De Flora et al., 2016). Pre-operative patients on PPIs at Duke University Hospital were fasted for a minimum of 7 h before sample collection. Collection of the GF was performed as a routine part of the standard pre-operative procedure, and was declared by the Duke Institutional Review Board to be research not involving human subjects. Samples were collected by laboratory personnel immediately after removal from the patient's stomach (just before thoracic surgery, after anesthesia was induced). Samples were stored from 12 to 32 min at room temperature (allowing time to collect more than one sample, to transport samples back to the laboratory, assess the pH and aliquot the sample or samples) before the samples were flash frozen with liquid nitrogen. To assess the effect of sample collection and handling on fed GF samples, a single vomit sample was collected from an ill individual, without induction, approximately 3 h following a meal. Use of this sample is exempt from IRB review in accordance with 45 CFR 46:101(4). Using the available human gastric samples, several *ex vivo* Cr(VI) reduction rate and capacity studies were conducted at Brooks Applied Labs (Bothell, WA) to evaluate the effect of GF dilution, stomach condition (fed vs. fasted), and pH as well as inter-individual variability in reduction and the presence of multiple reducing pools in the human GF samples. Control samples were also used in each experiment and consisted of 0.7% hydrochloric acid (HCl) in deionized (DI) water.

All samples were analyzed for Cr(VI) and Cr(III) using Speciated Isotope Dilution Mass Spectrometry (SIDMS) at Applied Speciation in Bothell, WA in accordance with the methods described in Proctor et al. (2012). Experimental design for each study is summarized in Table 1. With the exception of Study 3, pH of the diluted sample was approximately the same as that of the undiluted sample (Table 1). The pH and Eh of each gastric sample were measured before and after dilution.

Cr(VI) reductive capacity of each human gastric sample was measured first, and then, the time-course studies of rate reduction were conducted. Using ion chromatography Inductively Coupled Plasma Mass Spectroscopy (IC-ICP-MS), Cr(VI) reductive capacity at 90 or 240 min in the human gastric samples [spiking concentrations of 0.1 to 10 mg/L Cr(VI)] were measured (Table 1). In this work we have extended the time course to include time points longer than 60 min for several reasons: (1) to provide a more accurate estimate of GF sample reduction capacities; (2) to permit characterization of Cr(VI) reduction when combined with very slow gastric transit times; and (3) to allow for characterization of the reduction of Cr(VI) as lumen material transits through the intestinal tract (e.g., small intestinal lumen).

After Cr(VI) reductive capacity was measured, SIDMS analyses were conducted to quantify reduction rate at 0.25 to 240 min (Table 1). As described in Proctor et al. (2012), Cr(VI) (sodium dichromate dihydrate or SDD, primarily as the naturally abundant isotope ^{52}Cr) was added to the diluted gastric sample at concentrations ranging from 0.04 to 10.6 mg/L Cr(VI) (Table 1). At each specified time point after spiking with SDD, a 1-10 μL sample was collected and enriched rare isotopes ^{53}Cr(VI) and ^{50}Cr(III) (Applied Isotope Technologies, Pittsburgh PA) were added. Based on SIDMS, the concentration of Cr(VI) that remained in the gastric sample from the SDD spike at each specific time point was determined.

For most of the time-course studies, a double-spike approach was used to provide information on multiple reducing pools present in GF. The first Cr(VI) spike was added at $t \approx 0$ min to characterize rate and capacity at approximately 0.25, 5, and 20 min under low concentration conditions (0.04-0.1 mg/L), then the second Cr(VI) spike was added at t = 30 min to characterize reduction kinetics at 90 and 150 min under high concentration conditions (1-10 mg/L) (Table 1).

Please cite this article as: Kirman, C.R., et al., Reduction of hexavalent chromium by fasted and fed human gastric fluid. II. *Ex vivo* gastric reduction modeling, Toxicol. Appl. Pharmacol. (2016), http://dx.doi.org/10.1016/j.taap.2016.07.002

Table 1
Studies of Cr(VI) reduction capacity measured by IC-ICP-MS in gastric fluids (GF) collected from human volunteers (fed and fasted) and pre-operative patients on PPIs (fasted).

						Capacity Studies			Time-Course Studies		
Study Number	Objective	Sample Type[1]	Samples ID	pH[3]	Dilution[3]	Volume of Gastric Fluid	Dilution[3]	Reaction Time	Cr(VI) Spike Concentrations	Volume of Gastric Fluid	Reaction Time	Nominal Cr(VI) Spike Concentrations[4]
1	Assess effect of gastric fluid dilution	Fed Human Pooled (n = 1)[2]	2, 4, 7, 12, 14, 16, 20	1.7	9:1 2:1	1 mL 2 mL	9:1 2:1	90	10 mg/L	1 mL 3 mL	0.5, 2, 5, 20, 60, 240 min	10 mg/L
2A	Assess inter-individual variation in fed samples	Fed Human Individual (n = 8)	14 16 2 4 7 20 12 2 22	2.0 2.5 2.0 3.5 2.0 2.0 2.0 5.8 1.8	9:1	0.5 mL 0.5 mL 0.5 mL 0.5 mL 0.3 mL 0.5 mL 0.5 mL 0.5 mL 0.5 mL	9:1	240	2.7 mg/L 3.5 mg/L 3.9 mg/L 1.9 mg/L 3.2 mg/L 2.0 mg/L 2.2 mg/L 3.9 mg/L 10 mg/L	0.3 mL	0.25, 5, 20, 90, 150 min	Initial = 0.1-1 mg/L 2.6-10.6 mg/L at 30 min
2B	Assess inter-individual variation in PPI samples	PPI Human, Individual (n = 3)	P2 P19 P21	5 6.0 7.5	9:1	0.3 mL	9:1	240	0.1 mg/L	0.3 mL	0.25, 5, 20, 90, 150 min	Initial = 0.1 mg/L 1.0 mg/L at 30 min 0.04 mg/L
2C	Assess inter-individual variation in fasted samples	Fasted Human, Individual (n = 5)	6	1.9	9:1	0.3 mL	9:1	240	3 mg/L	0.3 mL	0.25, 5, 20, 90, 150 min	Initial = 0.1 mg/L 2.6 mg/L at 30 min
			11 15 17 19	1.6 2.5 1.6 1.6							0.25, 5, 20, 90, 150 min	Initial = 0.1 mg/L 1.5 mg/L at 30 min
3	Assess pH dependence	Fed Human, Individual (n = 1, evaluated at three pH levels)	2	2.0[4], 4.7, 5.8	9:1	0.3 mL	9:1	240	0.1 mg/L	0.3 mL	0.5, 5, 20, 60, 120 min	0.04 mg/L

[1] For each study, a control sample was used and consisted of 0.7% HCl and DI water. Fed and fasted GF samples were collected from 8 individuals; hence, 5 fasted human individuals in Experiment 2C are actually a subset of 8 fed individuals.
[2] In Study 1, two pooled samples of different dilutions (2:1 or 9:1) were tested. The pooled samples consisted of fed gastric fluids from 7 volunteers as noted in the "Sample Used" column.
[3] For all experiments except Experiment 3, dilutions of gastric samples were made using mixtures of HCl plus DI water to maintain the natural pH of undiluted gastric fluid or content.
[4] Sample at pH = 2 reflects naïve, unadjusted sample from experiment 2A.

2.2. Experimental Design

Using the analytical methods described above, a series of experiments was conducted for the purposes of better characterizing the reduction of Cr(VI) by human GF samples (Table 1). Each experiment is summarized briefly below.

2.2.1. Experiment 1: Effect of Dilution. As described previously (Proctor et al., 2012), GF is a viscous fluid that requires dilution to achieve a consistency that allows for homogenization and analysis, and data collected previously were done using a 9:1 dilution. To ensure that this dilution is properly accounted for in the reduction model, time course data were collected for up to 240 min to describe the reduction of Cr(VI) by a pooled GF sample (fed) from seven individuals (GF collected within a few hours post-meal). GF samples were diluted either 9:1 or 2:1 with mixtures of DI water and HCl to maintain the natural pH of the pooled sample (pH 1.7). The data collected from this experiment were then modeled with a 3-pool pharmacokinetic model (see Pharmacokinetic Modeling section below) with Cr(VI) concentration expressed one of two ways: (1) in terms of the *in vitro* assay conditions (i.e., mg/L diluted GF); and (2) in terms of GF volume (i.e., mg/L GF).

2.2.2. Experiment 2: Characterization of Inter-Individual Variation. Time course data were collected for up to 240 min to describe the reduction of Cr(VI) by individual fed or fasted GF samples (Experiments 2A and 2C; Table 1) and from fasted PPI users (Experiment 2B; Table 1). GF samples were diluted 9:1 with DI water and HCl to maintain the natural pH of the pooled sample. The data collected from this experiment were then modeled in a step-wise manner using 1-, 2-, and 3-pool reduction models. Pools were defined as either first [dependent only on Cr(VI) concentration] or second order [dependent on Cr(VI) and reducing agent concentration] reactions (see Pharmacokinetic Modeling section). To determine the number of pools required to provide the best overall fit, the modeling approaches were compared to assess model fit to the data using Akaike information criterion (AIC; see Pharmacokinetic Modeling section).

2.2.3. Experiment 3: Characterization of pH Dependence. Time course data were collected for up to 240 min to describe the reduction of Cr(VI) by GF samples from a single individual (GF collected approximately 1.5 h post-meal) at native pH (pH 2; sample 2 from experiment 2A; Table 1), and using the same sample with manually elevated pH levels (pH 4.7 and 5.8). GF samples were diluted 9:1 with DI water and HCl to achieve the desired pH levels. Values for the reduction rate constants (see Pharmacokinetic modeling section) were estimated separately for each pH value, and restricting the initial RE concentration to the same value in the model for all three simulations. To facilitate comparison of pH-dependent behavior across data sets, rate constant values were expressed as a fraction of the value obtained at native pH.

De Flora et al. (2016) assessed the amount of Cr(VI) reduced in 60 min by a single sample (native pH 2), with pH adjusted manually to pH values of 2.5, 4, 5, 6, 7, and 8. Changes in the amount of Cr(VI)

Please cite this article as: Kirman, C.R., et al., Reduction of hexavalent chromium by fasted and fed human gastric fluid. II. *Ex vivo* gastric reduction modeling, Toxicol. Appl. Pharmacol. (2016), http://dx.doi.org/10.1016/j.taap.2016.07.002

reduced in 60 min were assumed to be due to changes in the reduction rate constants (i.e., reducing equivalents was assumed constant for all pH values). Again, rate constant values were expressed as a fraction of the value obtained at native pH.

Three published data sets for likely GF reducing agents (glutathione, ascorbate, ferrous iron) were identified for characterizing the pH dependence of Cr(VI) reduction across a range of pH value spanning at least three pH units. These data sets include: (1) rate constants estimated from published time course data for Cr(VI) reduction by glutathione (Wiegand et al., 1984); (2) published rate constants for Cr(VI) reduction by ascorbate; and (3) published rate constants for Cr(VI) reduction by ferrous iron (Buerge and Hug, 1997). Time-course data (up to 120 min) for Cr(VI) reduction by glutathione were generated at pH values of 3, 4, 5, 6, 7, 7.4, and 8, and data were obtained by digitizing the figures of Wiegand et al. (1984) using GraphClick (version 3.0.3). Rate constants for each pH value were determined using a single-pool (i.e., only GSH present) reduction model. Rate constants for the reduction of Cr(VI) by ascorbate were measured from pH values of approximately 3.5 to 8.8 for several different temperatures (17.85 – 35.1 degrees Celsius; Dixon et al., 1993). Rate constant values collected at pH 8 and above were excluded because they were not considered relevant for normal gastric conditions. The behavior of the pH dependence was consistent across all temperatures; however, the magnitude of the rate constants was clearly temperature-dependent (higher rate constants at higher temperatures). For this reason, the rate constant values were pooled across temperatures by normalizing all values and expressing them as a fraction of the maximum value estimated at pH 3.5 for each temperature. Rate constants for the reduction of Cr(VI) by ferrous iron were measured from pH values of approximately 0.42 to 7.2 (Buerge and Hug, 1997).

Data from Experiment 3 (Table 1) and from De Flora et al. (2016) for GF were modeled using a 3-pool reduction model, while published data for single reductants were modeled using a 1-pool model. For all models, it was assumed that pH dependence is due to effects on the rate constant [or Cr(VI) predominance], and that the reducing agent pools are independent of pH. For the 3-pool reduction model, it was also assumed that the relationship between Cr(VI) reduction and pH is the same for all three reducing agent pools (i.e., pH-dependent curves for k1, k2, and k3 are parallel). These simplifying assumptions were necessary to obtain unique solutions and to ensure convergence during model optimizations. Several pH-dependent relationships (log-linear, piecewise log-linear, predominance) for the reduction rate constants were evaluated, as described below.

2.3. Log-linear (Original Model)

Kirman et al. (2013) proposed a simple, log-linear model to describe pH-dependence for a limited set of *ex vivo* reduction data:

$$Log(k) = m * pH + b \quad (6)$$

Where,

m = slope
b = intercept at pH 0

2.4. Piecewise Log-linear

As discussed by Kirman et al. (2013) the log-linear model may be an oversimplification in that "*the pKa for chromate (5.9) might serve as an inflection point for a nonlinear pH dependence of Cr(VI) reduction*". For this reason, a piecewise log-linear model was included in this evaluation:

$$\begin{aligned} Log(k) &= m1 * pH + b1; if\ pH <= P \\ Log(k) &= m2 * pH + b2; if\ pH > P \end{aligned} \quad (7)$$

Where,

m_1 = slope at low pH
b_1 = intercept at low pH
m_2 = slope at high pH
b_2 = intercept at high pH
P = inflection point between low and high pH

Two forms of the piecewise log-linear model were considered: (1) one in which the inflection point, P, is restricted to the published value for pK_{11} of 5.89 (Brito et al., 1997); and (2) another in which P was unrestricted, and optimized to fit the available data sets.

2.5. Cr(VI) Predominance

As stated in the introduction, the form of Cr(VI) present in aqueous media is pH dependent (Fig. 2A). Schlosser and Sasso (2014) proposed to relate reduction of Cr(VI) to the form of Cr(VI) present at a given pH. For comparing the behavior of this approach with the other approaches, their equations were adapted as follows:

$$k = K * \left(\left[H_2CrO_4 + HCrO_4^- + f \cdot CrO_4^{2-} \right) / Total\ Cr \right] \quad (8)$$

Where,

K = rate constant (k1, k2, or k3) at pH 0
f = fraction of activity attributed to CrO_4^{2-}

For the predominance model, the parameter K_{11} (Eq. (2)) determines the pH at which reduction reactivity decreases (analogous to parameter P in Eq. (7)). In this way, the rapid Cr(VI) reduction at low pH (below pK_{11}) is determined by the product, $K^*[H_2CrO_4 + HCrO_4]$, while slow reduction at high pH is determined by the product, $K^*f^*[CrO_4^{2-}]$ (Fig. 2B). The pH dependence of this model is determined by the value selected for pK_{11}. Similar to the approach used by Schlosser and Sasso (2014), two forms of the predominance model were included: (1) one in which the pK_{11} is restricted to its published value of 5.89 (Brito et al., 1997); and (2) another in which the pK_{11} term was unrestricted, and optimized to fit the available data sets.

2.6. Pharmacokinetic Modeling

2.6.1. Modeling to Evaluate the Number of Reducing Agent Pools. To evaluate the number of reducing agent pools present in GF samples, a total of six different forms reduction model were applied to the *ex vivo* GF data. These reduction models differed with respect to the number of reducing agent pools (n = 1 to 3) and the order of the reaction (1st or 2nd order):

1-Pool Models:

$$ReductionRate\ (1st\ orderreaction) = Cr(VI) * (k1) \quad (9)$$

$$ReductionRate\ (2nd\ orderreaction) = Cr(VI) * (k1 * RE1) \quad (10)$$

2-Pool Models:

$$ReductionRate\ (one\ 1st\ and\ one\ 2nd\ orderreactions) = Cr(VI) * (k1 * RE1 + k2) \quad (11)$$

$$ReductionRate\ (two\ 2nd\ orderreactions) = Cr(VI) * (k1 * RE1 + k2 * RE2) \quad (12)$$

Please cite this article as: Kirman, C.R., et al., Reduction of hexavalent chromium by fasted and fed human gastric fluid. II. *Ex vivo* gastric reduction modeling, Toxicol. Appl. Pharmacol. (2016), http://dx.doi.org/10.1016/j.taap.2016.07.002

3-Pool Models

$$ReductionRate\ (one\ 1st\ and\ two\ 2nd\ orderreactions) = Cr(VI)*(k1*RE1+k2*RE2+k3) \quad (13)$$

$$ReductionRate\ (three\ 2nd\ orderreactions) = Cr(VI)*(k1*RE1+k2*RE2+k3*RE3) \quad (14)$$

Where,

Cr(VI) = concentration of hexavalent chromium (mg/L)
k1 = 1st or 2nd order rate constant (fast reaction)
k2 = 1st or 2nd order rate constant (slow reaction)
k3 = 1st or 2nd order rate constant (very slow reaction)
RE1 = concentration of reducing equivalents (mg/L, pool 1, fast)
RE2 = concentration of reducing equivalents (mg/L, pool 2, slow)
RE3 = concentration of reducing equivalents (mg/L, pool 3, very slow)

The primary difference between the 1st and 2nd order reactions is that the rate of the 2nd order reactions is decreased as capacity of the reducing agents become depleted (i.e., RE concentration approaches zero). Optimizations for the reduction models were performed by adjusting the values for k (via the different pH-dependent equation parameters) and RE to maximize the model log-likelihood (LL) assuming the error terms for the model are normally distributed.

$$LL = -\frac{n}{2}\ln(2\pi) - \frac{n}{2}\ln\sigma^2 - \frac{1}{2\sigma^2}\sum_{i=1}^{n}(x_i-\mu)^2. \quad (15)$$

Variance was assumed to be proportionate to the mean based on an evaluation of duplicate sample data (CV = 3%). Comparison of model performance to the available data was assessed using AIC, calculated as:

$$AIC = 2*n - 2*LL \quad (16)$$

Where,

AIC = Akaike information criterion
n = number of estimated model parameters
LL = log likelihood function

For data sets in which optimal fits were difficult to obtain, the value for the concentration of Cr(VI) at time zero was allowed to vary by up to 20% to reflect uncertainty in starting conditions, consistent with the approach used by Schlosser and Sasso (2014).

2.6.2. Global Modeling. Data from all GF experiments (1-3), as well as from previously published data sets for pooled fed human GF samples (Kirman et al., 2013), yielding a total of 23 data sets, were modeled simultaneously using the number of reduction pools and pH dependence as indicated by Experiments 1-3. After optimization, the capacity of each reducing agent pool was characterized for fed and fasted individuals (i.e., means and standard deviations). The global model was then applied to time course data for Cr(VI) reduction by mouse and rat GF samples from Proctor et al. (2012) (see Supplement 2), and reduction capacities for each reduction pool were calculated. Three data sets (one each for mouse, rat, and human GF) were withheld from global model parameterization, and were used instead for the purpose of model validation. Model predictions were compared graphically to these data sets to assess the magnitude and behavior of the predictions.

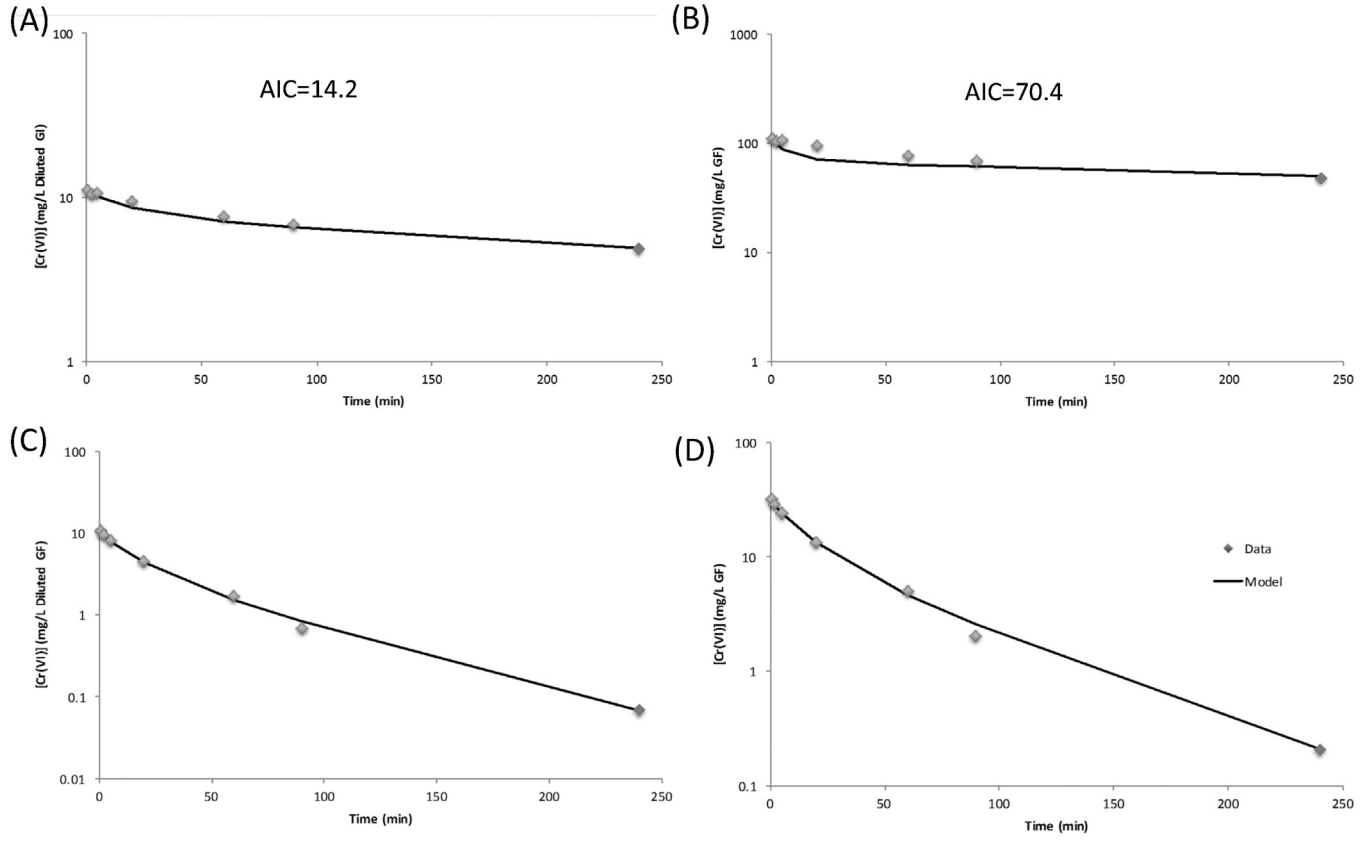

Fig. 3. Assessment of reduction models fit to human fed pooled sample at two different dilutions to determine appropriate units for expressing Cr(VI) concentration (Experiment 1): (A) 9:1 dilution modeled with concentration expressed in terms of per L diluted GF; (B) 9:1 dilution modeled with concentration normalized to per L GF (same data as in panel A, but normalized concentrations are 10x higher); (C) 2:1 dilution modeled with concentration expressed in terms of per L diluted GF; (D) 2:1 dilution modeled with normalized to per L GF (same data as in panel C, but normalized concentrations are 3x higher). Diamonds = time-course data points as measured by SIDMS; Solid line = reduction model fit to the data.

Please cite this article as: Kirman, C.R., et al., Reduction of hexavalent chromium by fasted and fed human gastric fluid. II. *Ex vivo* gastric reduction modeling, Toxicol. Appl. Pharmacol. (2016), http://dx.doi.org/10.1016/j.taap.2016.07.002

Table 2
Modeling Individual Data Sets: Evaluation of Reduction Model Complexity [Number of Cr(VI) Reducing Agent Pools] in Human GF Samples.

		Reducing Agent Pools					
Sample Group	Number of Reducing Agent Pools	Pool 1 (fast)	Pool 2 (slow)	Pool 3 (very slow)	Maximum LL For All Samples	Number of Estimated Parameters (each sample optimized individually)	AIC
Experiment 2A (n = 8 human fed samples)	1	1st order	NA	NA	-2452	8	4921
		2nd order	NA	NA	-782	16	1597
	2	2nd order	1st order	NA	-18	22	79
		2nd order	2nd order	NA	6	30	48
	3	***2nd order***	***2nd order***	***1st order***	***88***	***32***	***-112***
		2nd order	2nd order	2nd order	88	40	-95
Experiment 2B (n = 3 human PPI samples)	1	1st order	NA	NA	-159	3	325
		2nd order	NA	NA	28	6	-44
	2	2nd order	1st order	NA	53	9	-89
		2nd order	2nd order	NA	75	12	-126.0
	3	***2nd order***	***2nd order***	***1st order***	***78***	***15***	***-126.3***
		2nd order	2nd order	2nd order	78	18	-120
Experiment 2C (n = 5 human fasted samples)	1	1st order	NA	NA	-3659	5	7328
		2nd order	NA	NA	-54	10	127
	2	2nd order	1st order	NA	-51	15	133
		2nd order	2nd order	NA	31	20	-22
	3	***2nd order***	***2nd order***	***1st order***	***42***	***25***	***-35***
		2nd order	2nd order	2nd order	33	30	-5

Bolded, italicized rows indicate the best fitting reduction model with the lowest AIC for each sample group.

3. Results

3.1. Experiment 1: Effect of Dilution

Reduction model with rate constant expressed in terms of unadjusted concentrations (e.g., on a diluted-GF basis) provided a better fit to the data than when concentrations were normalized to GF volume (AIC values of 14.2 vs. 70.4; Fig. 3). These results are consistent with a chemical reaction that is dependent upon the concentration of Cr in the reaction vessel (e.g., mg Cr/L diluted GF), and thus, there is no need to normalize concentrations to GF volume (e.g., mg Cr/L GF) as was done for the previous version of the reduction model (Kirman et al., 2013). Based upon these results, a diluted-GF basis was identified as the best approach for the modeling work described below (Global Modeling section).

3.2. Experiment 2: Identification of the Number of Reducing Agent Pools

Reduction models with 1 to 3 reducing agent pools were applied to time course data collected using GF samples from fed volunteers, fasted volunteers, and PPI users. A comparison of model AIC values is provided in Table 2. For all three sample groups (fed, fasted, and PPI), the three-pool model, with the first two pools as 2nd order reactions, and third pool as a 1st order reaction (i.e., Eq. (13)) provided the best overall fit to the data. Fits for the best-fitting model are depicted in Fig. 4. Using the dual spike approach, evidence of multiple pools is clearly evident in these figures for samples in which the slope of time course data after the low-concentration spike (time points 0-30 min) is substantially steeper than the slope of the time course data after the high-concentration spike (time points >30 min). A similar conclusion was made for the presence of three pools in mouse and rat GF samples (Supplement 2), consistent with the results of Schlosser and Sasso (2014). Based upon these results, a three-pool model (Eq. (13)) was identified as the best choice for the global modeling work described below (Global Modeling section).

3.3. Experiment 3: Characterization of pH Dependence

Fits for a three-pool reduction model applied the data collected in Experiment 3 data are depicted in Fig. 5A-C. Inspection of the k values obtained from Experiment 3 does not suggest the presence of an inflection point between pH 2.0 and pH 5.8 (Fig. 5D). Because all three data points from this experiment fall below a pH of 5.89 for chromate, the piecewise log-linear 1 model cannot be used (reduces to the log-linear model). The predominance 2 model (optimized $pK_{11} = 3.11$) provided the best overall fit to the data (Table 3; Fig. 5D). However, in order to fit the *ex vivo* data collected across pH levels, this model requires (1) shifting the value for K_{11} by more than 2 orders of magnitude (optimized pK_{11} of 3.11 vs. published value of 5.89); and (2) that the k values obtained at pH 2 and 5.8 for Experiment 3 are at their respective maximum and minimum values, respectively (i.e., plateaus predicted at pH<2 and pH>5.8). The log-linear model and piecewise log-linear model 2 (optimized inflection point, P = 5.46) also perform reasonably well with these data. The predominance model 1 (pK_{11} fixed at 5.89) provided a poor to fit these data, largely because it predicts a constant value (i.e., plateau) for the reduction constant below pH 5.

Please cite this article as: Kirman, C.R., et al., Reduction of hexavalent chromium by fasted and fed human gastric fluid. II. *Ex vivo* gastric reduction modeling, Toxicol. Appl. Pharmacol. (2016), http://dx.doi.org/10.1016/j.taap.2016.07.002

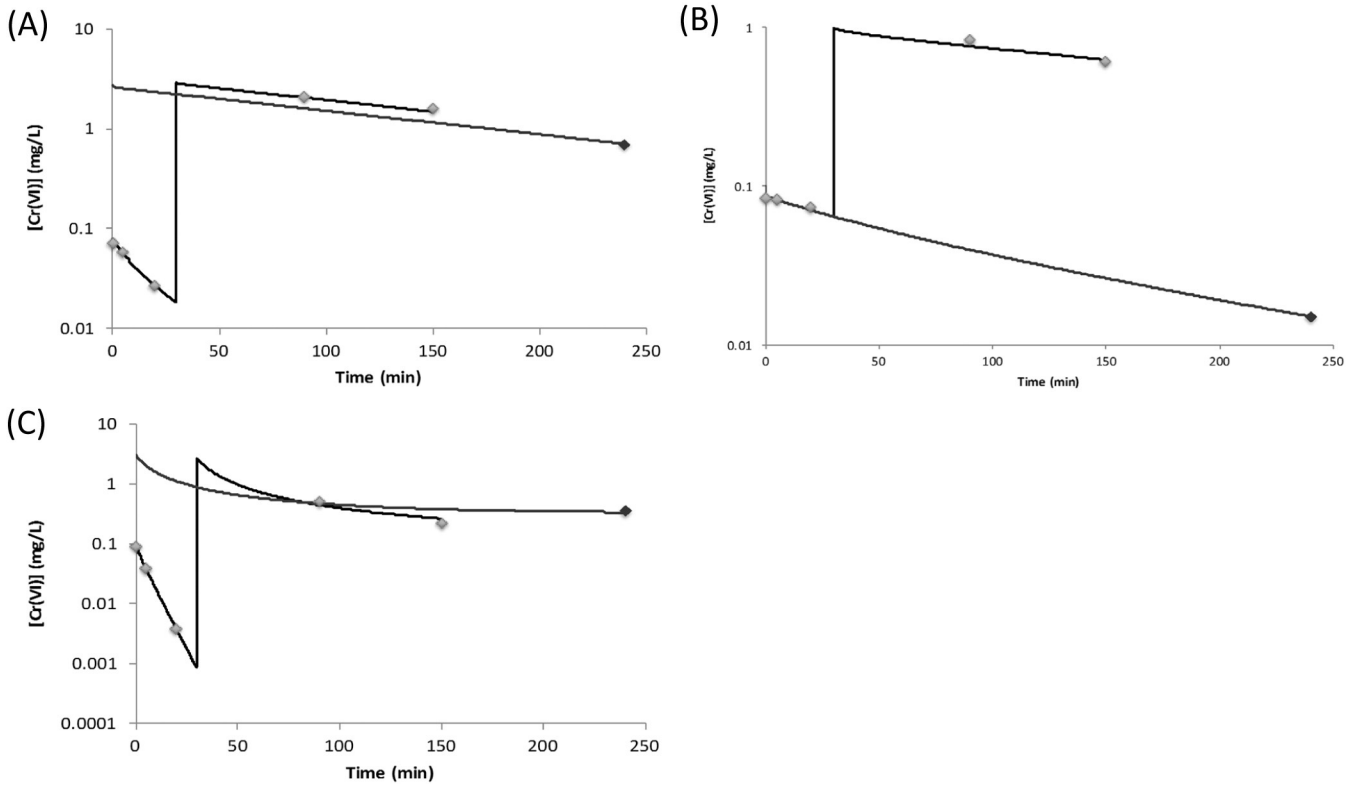

Fig. 4. Fits of a 3-pool reduction model applied to separately to example data sets from (A) a Fed GF Sample; (B) a PPI-User GF Sample; and (C) a Fasted GF Sample (fits to all data sets are provided in Supplement 1). Dark diamonds = time-course data points as measured by SIDMS for capacity runs(t = 240 min); Light diamonds = time-course data points as measured by SIDMS (t = 0-90 min); Solid lines = reduction model predictions.

Fits for a three-pool reduction model applied the data collected by De Flora et al. (2016) are depicted in Fig. 6A. Inspection of the pH-dependent behavior for k values obtained from these data does not suggest the presence of a strong inflection point between pH 2.0 and pH 8.0. The piecewise log-linear model 2 (optimized P = 4.3) provided the best overall fit to the data (Table 3; Fig. 6A). The piecewise log-linear model 1 (P fixed at 5.89) also performs reasonably well with these data. Both forms of the predominance model provided a poor fit these data.

A comparison of the optimized pH-dependent model forms applied to the glutathione rate constants obtained from Wiegand et al. (1984) time course data is depicted in Fig. 6B. For these time course data, the piecewise log-linear model 2 with pH (optimized P = 5.7) provided the best overall fit (Table 3). The optimized value for the inflection point is fairly consistent (within half a pH unit) with the published pK_{11} value of 5.89. The log-linear model performs poorly for this data set, because it fails to capture the nonlinear behavior (i.e., inflection point). Both forms of the predominance model perform poorly for these data because their predicted behavior for reduction rate constant (e.g., presence of plateaus) does not agree with the behavior needed to fit the time course data.

A comparison of the optimized pH dependent model forms applied to the ascorbate rate constants reported by Dixon et al. (1993) is depicted in Fig. 6C. For these data, the piecewise log-linear model 2 (optimized P = 6.19) provided the best overall fit (Table 3). In this case, the optimized value for P is consistent (within half a pH unit) with the published pKa value for chromate (5.89). Both forms of the predominance model perform reasonably well for this data set. However, the log-linear model performs poorly because it fails to capture the nonlinear behavior (i.e., apparent inflection point near pH 6).

A comparison of the optimized pH dependent model forms applied to the reduction rate constants reported for ferrous iron by Buerge and Hug (1997) is depicted in Fig. 6D. The pH-dependent behavior noted for ferrous iron is clearly different than that observed for the other data sets (i.e., apparent "U" shape). For these data, the piecewise log-linear model 2 (optimized P = 4.3) provided the best overall fit (Table 3). The optimized value for the inflection point is considerably lower than the published pKa value for chromate (5.89). Due to the unusual behavior of these data, all other models perform poorly.

Overall, the piecewise log-linear model 2 (with optimized inflection point, P) provided the best fit for 4 of 5 data sets, and nearly provided best fit for the remaining data set. For this reason, this form of the reduction model was identified as the best choice for modeling pH dependence in the modeling work described below (Global Modeling section).

3.4. Global Modeling

These results described above for Experiments 1, 2 and 3 were used to guide the form of the global reduction model applied to all GF data sets. Based upon these results, the data were modeled by expressing Cr(VI) concentrations in terms of the diluted-GF basis (Experiment 1), a three-pool reduction model was used (Experiment 2), and the pH-dependence was defined using a piecewise log-linear model 2 (Experiment 3).

Optimized fits of the global model to all data sets (Experiments 1, 2, and 3, plus the data sets from Kirman et al., 2013) are provided in Supplement 1. Based upon the combined *ex vivo* data set, the piecewise log-linear model 2 yielded an optimized inflection point (P) of 5.3, with a shallower slope indicated above this pH value (Fig. 7). The resulting formulas for calculating pH-dependent reduction rate constants (k1, k2, k3; Eq. (13)), as well as values for reducing equivalent concentrations for each pool (RE1, RE2, RE3; Eq. (13)) are summarized in Table 4. The predicted concentration of reducing equivalents in pool 1 (RE1) is greater in fasted samples than in fed samples (2.7 vs. 0.70 mg/L), while the

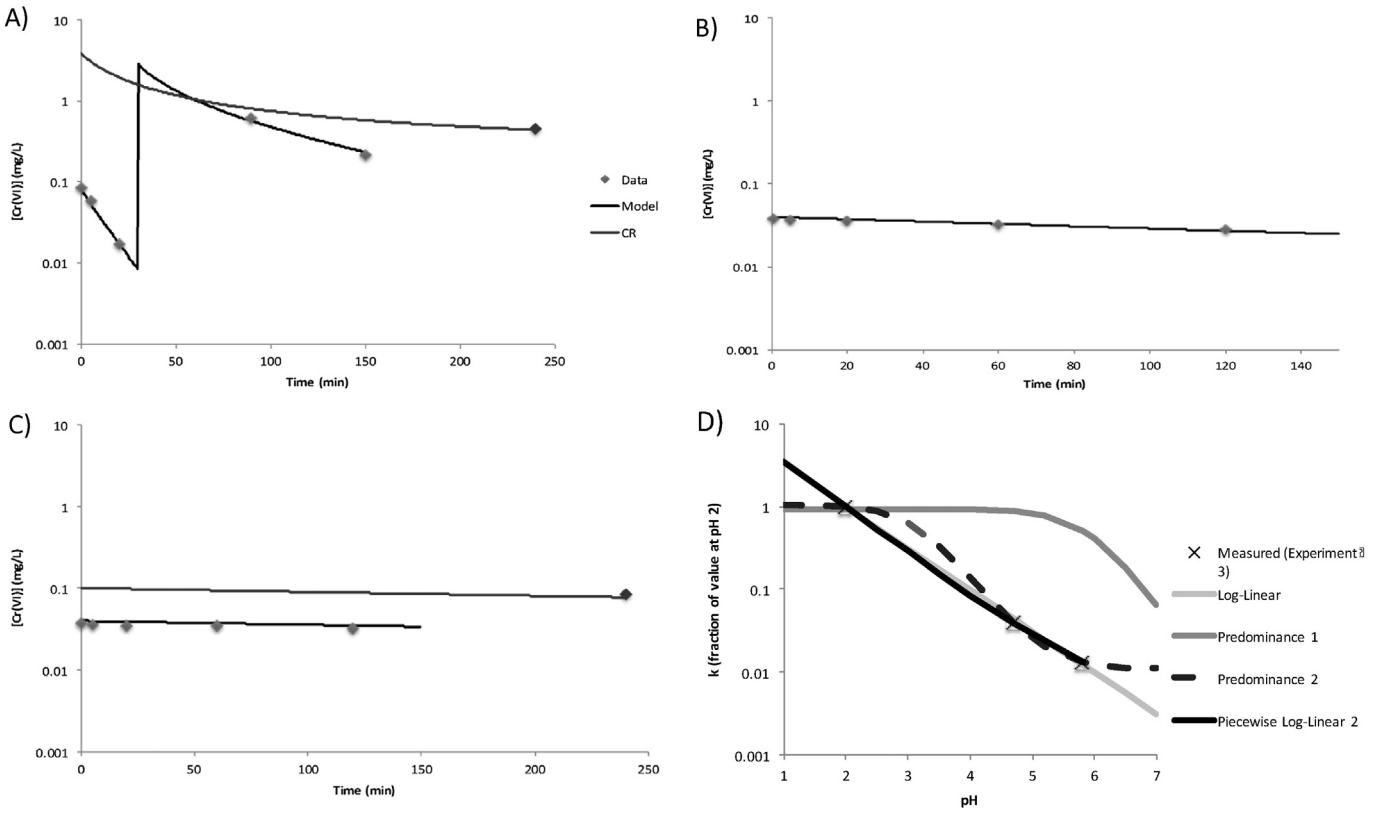

Fig. 5. Assessing the pH dependence for Cr(VI) reduction rate constants using data from Experiment 3: A) Three pool model fit to data from Experiment 3A (native pH = 2); B) Three pool model fit to data from Experiment 3A (adjusted pH = 4.7); C) Three pool model fit to data from Experiment 3A (adjusted pH = 5.8); Dark diamonds = time-course data points as measured by SIDMS for capacity runs(t = 240 min); Light diamonds = time-course data points as measured by SIDMS (t = 0-90 min); Solid lines = reduction model predictions; D) Alternative pH-dependent model forms fit to the data in panels 5A-C. X's = rate constant values obtained from fit time-course data in panes A-C; Lines = different pH-dependent relationship predictions for the reduction rate constant.

reverse is observed for pool 2 (13 vs. 27 mg/L). In rodents, reducing equivalents are generally higher in rats than mice (Table 4; Supplement 2). Predictions made by the global reduction model for the three validation data sets (one for each species) are fairly consistent with the behavior of the data (Fig. 8), with a slight tendency to overestimate the amount of Cr(VI) left at the late time points, but in all cases the predicted concentrations for Cr(VI) are within a factor of two of the measured values.

4. Discussion

A series of experiments were conducted to support pharmacokinetic modeling of Cr(VI) reduction. These data help address data gaps and limitations with respect to (1) the expression of Cr(VI) concentrations in the model; (2) the reduction of Cr(VI) in fed human GF samples; (3) the number of Cr(VI) reduction pools present in human fed, fasted, and PPI-user GF samples; and (4) an appropriate form for the pH

Table 3
Evaluation of pH-Dependent Model Forms for Cr(VI) Reduction.

				AIC for Model Form				
Data Set	pH Range	Reducing Agent	Number of Pools Included	Log-linear	Predominance 1 (Inflection point fixed at pH 5.88)	Predominance 2 (Inflection point optimized, value in parentheses)	Piecewise Log-linear 1 (Inflection point fixed at pH 5.89)	Piecewise Log-linear 2 (Inflection point optimized, value in parentheses)
Time-Course Data for Adjusted pH Sample (Experiment 3)	2-5.8	Gastric Fluid	3	-11	2,034	***-25 (3.2)***	-11 (reduces to log-linear model)	-23 (5.5)
Time-Course Data for Adjusted pH Sample (De Flora et al., 2016)	2-8	Gastric Fluid	3	33	480	55 (3.7)	-19	***-29 (4.3)***
Time-Course Data (Wiegand et al., 1984)	3-8	Glutathione	1	15,978	17,247	15,044 (5.0)	14,729	***14,710 (5.7)***
Reduction Rate Constants (Dixon et al., 1993)	3.53-7.9	Ascorbate	1	22,590	5,358	4,604 (5.8)	4,954	***4,510 (6.1)***
Reduction Rate Constants (Buerge and Hug, 1997)	0.4 – 7.1	Iron(II)	1	18416	19068	17311 (0.0)	13608	***4671 (4.3)***

Bolded, italicized values indicate the best fitting model with the lowest AIC value.

Please cite this article as: Kirman, C.R., et al., Reduction of hexavalent chromium by fasted and fed human gastric fluid. II. *Ex vivo* gastric reduction modeling, Toxicol. Appl. Pharmacol. (2016), http://dx.doi.org/10.1016/j.taap.2016.07.002

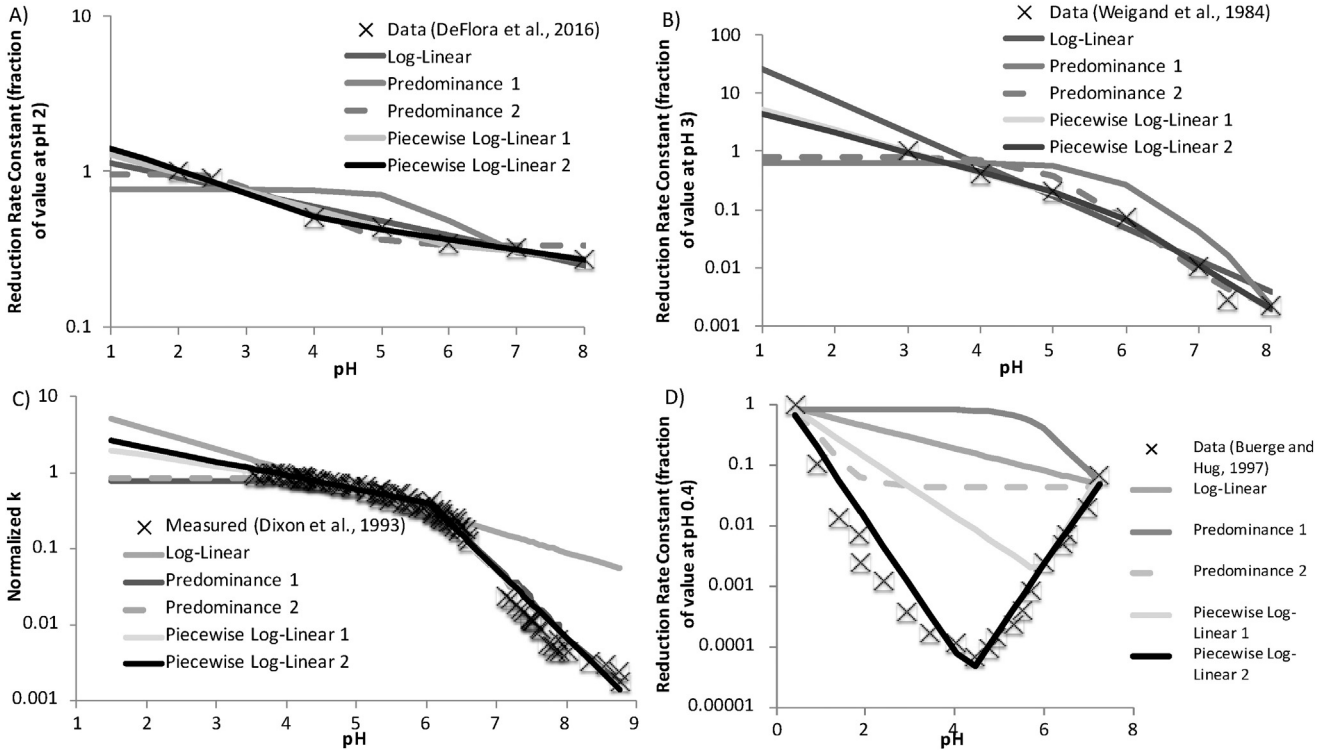

Fig. 6. Assessing the pH dependence for Cr(VI) reduction rate constants using data from published data sets for GF (De Flora et al., 2016), glutathione (Wiegand et al., 1984), ascorbate (Dixon et al., 1993), and Iron(II) (Buerge and Hug, 1997): A) Comparison of pH-dependent forms for reduction rate constant optimized to fit GF data (De Flora et al., 2016); B) Comparison of pH-dependent forms for reduction rate constant optimized to fit glutathione time-course data (Wiegand et al., 1984); C) Comparison of pH-dependent forms for reduction rate constant optimized to fit published rate constants for ascorbate (Dixon et al., 1993); D) Comparison of pH-dependent forms for reduction rate constant optimized to fit published rate constants for iron(II) (Buerge and Hug, 1997); X's = normalized rate constant values (relative to value at pH = 2) used to fit time-course data in panes A-C; Lines = different pH-dependent relationship predictions for the reduction rate constant.

dependence for Cr(VI) reduction. As such, the revised modeling results herein provide improved characterization of Cr(VI) gastric reduction kinetics as compared to the original model in Kirman et al. (2013) and the Schlosser and Sasso (2014) model.

In this study of human GF samples, we have specifically utilized a dual spike approach to examine the presence of multiple reducing agent pools in human GF samples under fed and fasted conditions, as well as with PPI use. Together the available data are consistent with the presence of three reducing agent pools being present in mouse, rat, and human GF samples (*i.e.*, there does not appear to be a species difference with respect to the number of reducing agent pools present). Use of a single pool model in previous work (Kirman et al., 2013; Schlosser and Sasso, 2014) reflected a limitation of the previous data set.

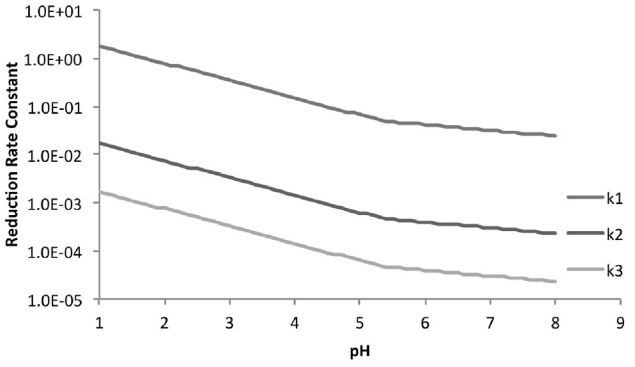

Fig. 7. pH dependent Cr(VI) reduction rate constants based upon global optimization of a three-pool, piecewise log-linear reduction model applied to all human time-course data from Experiment 2A-C (optimized inflection point at pH = 5.3).

The reduction capacity of fed human samples, as estimated by summing the reducing equivalents concentrations for pools 1 and 2 (approximately 28 mg/L), is consistent with the data generated by De Flora et al. (2016) using the DPC method in which reduction capacity was 20.4 ± 2.61 mg/L in post-meal samples. These results are also comparable to previous capacity measures by De Flora et al. (1987). Because the precise time between meal consumption and GF sample collection for the fed samples used in this study is not known, a better comparison would be to compare the reduction capacity estimate of 28 mg/L to a time-weighted average of the capacity measured up to a few h post meal by De Flora et al. (1987), which is expected to fall somewhere between 10 mg/L and 60 mg/L. With respect to reduction capacity fasted samples, the values derived here (approximately 16 mg/L) is moderately higher than that reported by De Flora et al. (1987) (8.3 ± 4.7 mg/L) and in De Flora et al. (2016) (10.3 ± 2.39 mg/L). These differences may reflect in part, differences in incubation times used to assess Cr(VI) reduction by GF (up to 240 min used here *vs.* 60 min used by De Flora et al.).

An empirical model (piecewise log-linear model 2) was used to characterize the pH-dependence of the reduction rate constants. This model is slightly more complex than the log-linear model used previously (Kirman et al., 2013), in that additional model parameters were introduced to permit an inflection point (P), as well as different slopes above and below this pH value, but remains relatively simple to implement. Alternative pH-dependent models were also considered, including the chemistry-motivated predominance model of Schlosser and Sasso (2014), but these generally struggled to fit some data sets. The behaviors of the different pH-dependent forms assessed for the Cr(VI) reduction rate constants differ with respect to their inflection point, as well as the presence or absence of plateaus. The plateau behavior predicted by the predominance models is driven by lumping of all forms of Cr(VI), other than CrO_4^{-2}, together (Fig. 2). Based upon the data

Please cite this article as: Kirman, C.R., et al., Reduction of hexavalent chromium by fasted and fed human gastric fluid. II. *Ex vivo* gastric reduction modeling, Toxicol. Appl. Pharmacol. (2016), http://dx.doi.org/10.1016/j.taap.2016.07.002

Table 4
Global Pharmacokinetic Modeling Results: Reduction Capacities (mean +/- SD, mg/L)

Species for GF Samples	Reducing Agent Pool (reaction rate)	pH Dependence Equation for Rate Constants	Reducing Equivalents Concentration (mg/L)	
			Fed	Fasted
Human	Pool 1 (fast)	*Log(k1) = -0.358*pH + 0.614; if pH<=5.63*	0.68 ± 0.76	2.6 ± 2.8
		*Log(k1) = -0.031*pH-1.226; if pH>5.63*		
	Pool 2 (slow)	*Log(k2) = -0.358*pH-1.415; if pH<=5.63*	27 ± 28	12 ± 18
		*Log(k2) = -0.031*pH-3.254; if pH>5.63*		
	Pool 3 (very slow)	*Log(k3) = -0.358*pH-2.431; if pH<=5.63*	Unlimited[1]	Unlimited[1]
		*Log(k3) = -0.031*pH-4.271; if pH>5.63*		
Mouse[2]	Pool 1 (fast)	Same as above (pH = 4.5)	6.1	NA
	Pool 2 (slow)		27	NA
	Pool 3 (very slow)		Unlimited[1]	NA
Rat[2]	Pool 1 (fast)	Same as above (pH = 4.38)	7.1	NA
	Pool 2 (slow)		73	NA
	Pool 3 (very slow)		Unlimited[1]	NA

NA = not applicable; rodent GF samples (Proctor et al., 2012) were collected under the conditions to match the NTP bioassay (NTP, 2008) in which rodents were fed *ad libitum*.
[1] Modeled as a first order reaction (no capacity term for reducing equivalents; Eq. (12))
[2] See modeling results in Supplement 2.

evaluated for pH dependence (Experiment 3 of this study; De Flora et al., 2016; Wiegand et al., 1984; Dixon et al., 1993; Buerge and Hug, 1997), there does not appear to be evidence to support the presence of plateaus in the pH-dependence for reduction rate constants, as predicted by the predominance model of Schlosser and Sasso (2014).

When simultaneously fit to all data sets, the piecewise log-linear model 2 predicts a shallower slope (above the inflection point, than observed below the inflection point (Fig. 7). This behavior differs from pH-dependent behaviors observed for glutathione (Fig. 6B) and ascorbate (Fig. 6C) assessed individually, where the slope observed at high pH is steeper that that observed at low pH. One explanation for this apparent difference in behavior may be the possible contribution of ferrous iron at high pH. Ferrous iron exhibits an unusual ("U" shapes) behavior with respect to Cr(VI) reduction (Fig. 6D). The study authors attributed this behavior due to the predominance of different forms of iron present at a given pH [e.g., Fe^{2+}, $FeOH^{+}$, $Fe(OH)_2$], each of which may have a different reaction rate with Cr(VI). Because dietary iron is predominantly as the ferric form, the concentration of ferrous iron in the stomach lumen is not expected to be high. Low concentrations of ferrous iron are possible given the redox state of GF, such that predominance of iron forms is in equilibrium with other reducing agents (sulfhydryls, ascorbate) present in GF. In the small intestinal lumen, however, due to the high activity of ferrous iron at high pH (Fig. 6D) and due to the reduction of ferric iron to ferrous iron (II) at the brush border of the small intestine (required for iron absorption), ferrous iron may play a much larger role in Cr(VI) reduction in the small intestinal lumen (Suh et al., 2014).

The predominance models (1 and 2) assessed in this work are relatively simple variations consistent with those proposed by Schlosser and Sasso (2014), but could be extended to be more complex. For example, instead of combining redox active forms of Cr(VI) (H_2CrO_4 and $HCrO_4^-$), different reduction activities could be attributed to each form [e.g., k = K* (H_2CrO_4 + f1*$HCrO_4$- + f2*$CrO_4$2-)/Total Cr]. In addition to the predominance of Cr(VI) forms, the data of Buerge and Hug (1997) indicate that the rate of reduction can also depend upon the predominance of the reducing agent forms [e.g., Fe2 +, FeOH +, Fe(OH)2]. The plateau behavior predicted by the predominance model could be eliminated by including a slope in place of the rate constant at pH 0 [e.g., k = (m*pH + b)* (H_2CrO_4 + f1*$HCrO^{4-}$ + f2*CrO_4^{2-})/Total Cr]. Such a model would be consistent with reduction models that include a role for hydrogen ion in some reduction reactions (Connett and Wetterhahn, 1983), but again would require increasing model complexity. It is not clear that such a complex model would provide a meaningful benefit over the comparatively simpler empirical model recommended here (piecewise log-linear model).

Sasso and Schlosser (2015) recently assessed the impact of alternative reduction models on resulting internal dose measures as predicted by a physiologically based pharmacokinetic model for Cr(VI) to support human health risk assessment. Despite using models that differ with respect to complexity (single pool vs. three pools) and pH dependence (e.g., log-linear vs. predominance 2 models), the authors reported very similar results (i.e., within a factor of 2) for the points of departure calculated for effects in the mouse small intestine as compared to those calculated by Thompson et al. (2014). In short, despite differences in model complexity, alternative models yield quite similar reduction rates. This is possible because the second order reduction rates are dependent on three terms [i.e., Cr(VI)*k*RE]. In this way, a model that predicts a low value for k can be consistent with a competing model that predicts a higher value for k at a given pH, provided that reciprocal changes are made for the RE terms (i.e., such that their products are the same). For this reason, the selection of the form of the pH dependence for k can have an indirect effect on the predicted values for reduction capacity.

The data and modeling presented here will be invaluable with respect to supporting pharmacokinetic modeling and human health risk assessment for Cr(VI). In particular, these data will be useful in characterizing: (1) internal doses in humans exposed to Cr(VI) during a meal;

Please cite this article as: Kirman, C.R., et al., Reduction of hexavalent chromium by fasted and fed human gastric fluid. II. *Ex vivo* gastric reduction modeling, Toxicol. Appl. Pharmacol. (2016), http://dx.doi.org/10.1016/j.taap.2016.07.002

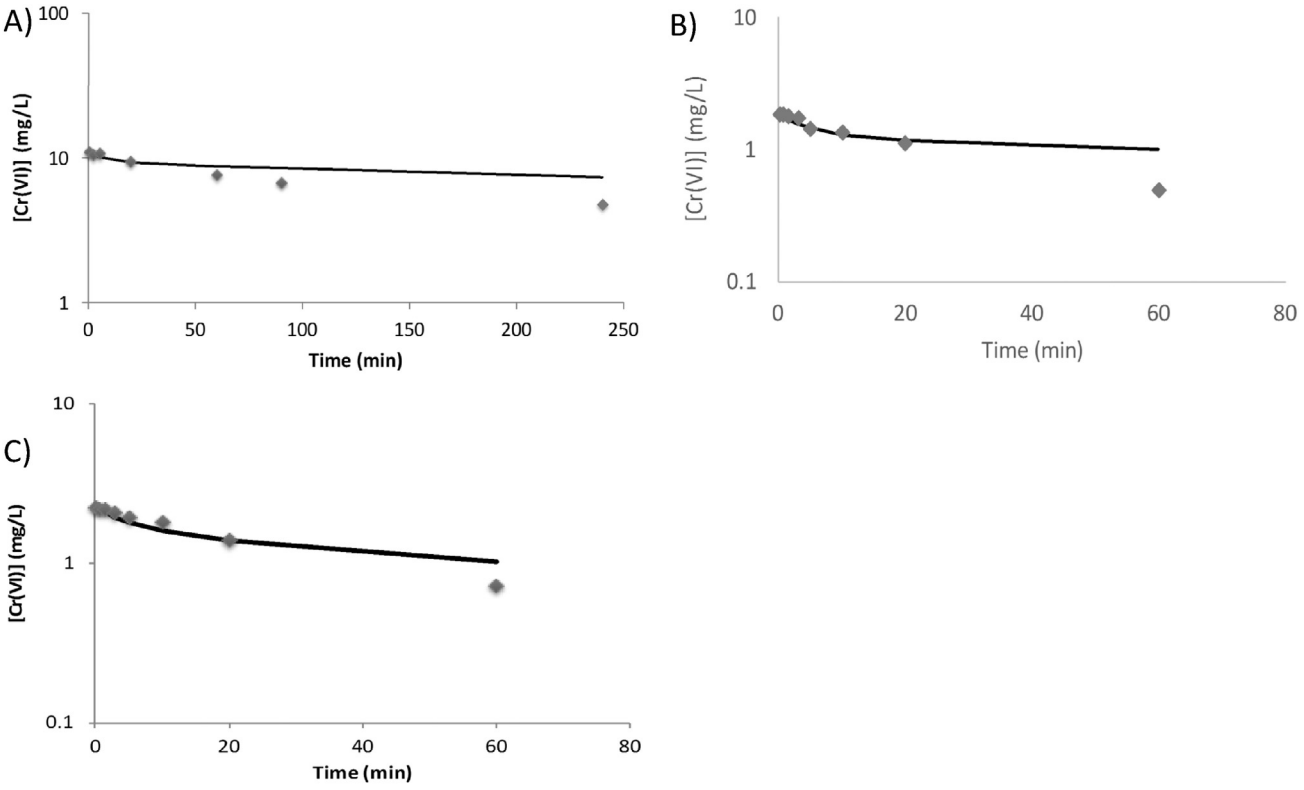

Fig. 8. Validation of the final reduction model (three-pool, piecewise log-linear model) using three data sets: A) Pooled fed human GF sample; B) Mouse GF sample; C) Rat GF sample.

(2) inter-individual variation in internal doses in humans for both fed and fasted states; and (3) inter-individual variation in a potentially sensitive subpopulation (e.g., neonates, PPI users). The presence of multiple pools in human GF, in particular, has important implications to low-dose risk predictions. Specifically, the presence of a fast but low capacity reduction reaction (RE pool 1; Eq. (13)) predicts a more efficient detoxification of Cr(VI) at low concentrations (e.g., below the capacity of pool 1), than at higher concentrations in which detoxification becomes dependent upon slower detoxification reaction rates (RE pools 2 and 3). The capacity of the pool 1 for fed conditions, which is lower than that for fasted conditions, is 0.7 mg/L, which far exceeds typical human drinking water exposure to Cr(VI) considering the federal maximum contaminant level is 0.1 mg/L, and recent drinking water exposure data for Cr(VI) collected by the US Environmental Protection Agency (USEPA) indicate that mean levels of Cr(VI) in drinking water across the US are less than 0.001 mg/L (USEPA, 1991, 2016). As such, at expected drinking water exposures, detoxification of Cr(VI) by reduction to Cr(III) should be rapid (less than 1 minute). Therefore, extrapolation of the cancer incidence observed in rodents exposed to very high concentrations of Cr(VI) to human populations exposed to low concentrations of Cr(VI) will need to quantify the dose-dependent, nonlinear toxicokinetics (i.e., sequential depletion of RE pools 1 and 2) in order to provide an accurate depiction of low-dose risks from Cr(VI) exposure, and will need to be able to quantify risk in sensitive subpopulations (e.g., neonates, PPI users).

Transparency document

The Transparency document associated with this article can be found, in online version.

Acknowledgements

Partial funding for this research was received by the Hexavalent Chromium [Cr(VI)] Panel of the American Chemistry Counsel (ACC). ACC did not contribute to the study design, data collection, analysis or interpretation of the data or preparation of the manuscript. ToxStrategies and Summit Toxicology continue to provide consulting services to ACC on related projects. Chad Thompson (ToxStrategies) reviewed and commented on the draft manuscript. The content and conclusions of the paper are solely those of the authors.

Appendix A. Supplementary data

Supplementary data to this article can be found online at http://dx.doi.org/10.1016/j.taap.2016.07.002.

References

Brito, F., Ascanio, J., Mateo, S., Hernández, C., Araujo, L., Gili, P., Martín-Zarza, P., Domínguez, S., Mederos, A., 1997. Equilibria of chromate(VI) species in acid medium and ab initio studies of these species. Polyhedron 16 (21), 3835–3846.

Buerge, I.J., Hug, S.J., 1997. Kinetics and pH Dependence of Chromium(VI) Reduction by Ferrous iron. Swiss Federal Institute for Environmental Science and Technology (EAWAG), CH-8600 Duebendorf, Switzerland. Environ. Sci. Technol. 31 (5), 1426–1432 (1997).

Connett, P.H., Wetterhahn, K.E., 1983. Metabolism of the carcinogen chromate by cellular constituents. Inorganic Elements in Biochemistry. Volume 54 of the series Structure and Bonding, pp. 93–124.

De Flora, S., 2000. Threshold mechanisms and site specificity in chromium(VI) carcinogenesis. Carcinogenesis 21 (4), 533–541.

De Flora, S., Camoirano, A., Micale, R.T., La Maestra, S., Savarino, V., Zentilin, P., Marabotto, E., Suh, M., Proctor, D.M., 2016. Reduction of hexavalent chromium by fasted and fed human gastric fluid. I. Chemical reduction and mitigation of mutagenicity. Toxicol. Appl. Pharmacol.

De Flora, S., Badolati, G.S., Serra, D., Picciotto, A., Magnolia, M.R., Savarino, V., 1987. Circadian reduction of chromium in the gastric environment. Mutat. Res. 192 (3), 169–174 (1987 Nov).

Dixon, D.A., Sadler, N.P., Dasgupta, T.P., 1993. Oxidation of biological substrates by chromium(VI). Part 1. Mechanism of the oxidation of L-ascorbic acid in aqueous solution. J. Chem. Soc. Dalton Trans. 3489–3495.

Kirman, C.R., Aylward, L.L., Suh, M., Harris, M.A., Thompson, C.M., Haws, L.C., Proctor, D.M., Lin, S.S., Parker, W., Hays, S.M., 2013. Physiologically based pharmacokinetic model for humans orally exposed to chromium. Chem. Biol. Interact. 204 (1), 13–27.

NTP, 2008. Toxicology and carcinogenesis studies of sodium dichromate dihydrate (Cas No. 7789-12-0) in F344/N rats and B6C3F1 mice (drinking water studies). NTP TR

546, NIH Publication No. 08-5887. National Toxicology Program, Research Triangle Park, NC, pp. 1–192.

Proctor, D.M., Suh, M., Aylward, L.L., Kirman, C.R., Harris, M.A., Thompson, C.M., Gurleyuk, H., Gerads, R., Haws, L.C., Hays, S.M., 2012. Hexavalent chromium reduction kinetics in rodent stomach contents. Chemosphere 89 (5), 487–493. http://dx.doi.org/10.1016/j.chemosphere.2012.04.065.

Sasso, A.F., Schlosser, P.M., 2015. An evaluation of in vivo models for toxicokinetics of hexavalent chromium in the stomach. Toxicol. Appl. Pharmacol. 287 (3), 293–298.

Schlosser, P.M., Sasso, A.F., 2014. A revised model of ex-vivo reduction of hexavalent chromium in human and rodent gastric juices. Toxicol. Appl. Pharmacol. 280 (2), 352–361.

Suh, M., Thompson, C.M., Kirman, C.R., Carakostas, M.C., Haws, L.C., Harris, M.A., Proctor, D.M., 2014. High concentrations of hexavalent chromium in drinking water alter iron homeostasis in F344 rats and B6C3F1 mice. Food Chem. Toxicol. 65, 381–388 (2014 Mar).

Thompson, C.M., Kirman, C.R., Proctor, D.M., Haws, L.C., Suh, M., Hays, S.M., Hixon, J.G., Harris, M.A., 2014. A chronic oral reference dose for hexavalent chromium-induced intestinal cancer. J. Appl. Toxicol. 34, 525–536.

USEPA, 1991. National primary drinking water regulations-synthetic organic chemicals and inorganic chemicals; monitoring for unregulated contaminants; national primary drinking water regulations implementation; national secondary drinking water regulations. Final rule. Fed. Regist. 56, 3526–3597.

USEPA, 2016. The Third Unregulated Contaminant Monitoring Rule (UCMR3): Occurrence Data. April https://www.epa.gov/dwucmr/occurrence-data-unregulated-contaminant-monitoring-rule#3.

Wiegand, H.J., Ottenwälder, H., Bolt, H.M., 1984. The reduction of chromium (VI) to chromium (III) by glutathione: an intracellular redox pathway in the metabolism of the carcinogen chromate. Toxicology 33 (3-4), 341–348 (1984 Dec).

Please cite this article as: Kirman, C.R., et al., Reduction of hexavalent chromium by fasted and fed human gastric fluid. II. *Ex vivo* gastric reduction modeling, Toxicol. Appl. Pharmacol. (2016), http://dx.doi.org/10.1016/j.taap.2016.07.002